

The structure of barium M-hexaferrite ($\text{BaFe}_{12-2x}\text{Co}_x\text{Ni}_x\text{O}_{19}$) powders using co-precipitation methods

Cite as: AIP Conference Proceedings **2251**, 040028 (2020); <https://doi.org/10.1063/5.0015750>

Published Online: 18 August 2020

Susilawati, Aris Doyan, Muhammad Taufik, and Wahyudi



View Online



Export Citation

ARTICLES YOU MAY BE INTERESTED IN

[Electrical properties of M-type barium hexaferrites \(\$\text{BaFe}_{12}\text{ZnMnO}_{19}\$ \)](#)

AIP Conference Proceedings **2251**, 040043 (2020); <https://doi.org/10.1063/5.0015695>

[A study of microstructure and shape memory properties in Cu-Zn-Al by miscellaneous cooling medium during martensite formation](#)

AIP Conference Proceedings **2251**, 040023 (2020); <https://doi.org/10.1063/5.0016174>

[Thermal cycling study of prospective fuel-cell sealants from silica-sand/alumina composites](#)

AIP Conference Proceedings **2251**, 040029 (2020); <https://doi.org/10.1063/5.0015633>

Lock-in Amplifiers
up to 600 MHz



The Structure of Barium M-Hexaferrite (BaFe_{12-2x}Co_xNi_xO₁₉) Powders Using Co-Precipitation Methods

Susilawati^{1, 2, *)}, Aris Doyan^{1, 2}, Muhammad Taufik¹, and Wahyudi¹

¹Physics Education, FKIP, University of Mataram, Lombok, West Nusa Tenggara, Indonesia.

²Master of Science Education Study Program, University of Mataram, West Nusa Tenggara, Indonesia.

*)Corresponding author: susilawatihambali@unram.ac.id

Abstract. Barium M-hexaferrite were synthesized with Co-Ni doping ions (BaFe_{12-2x}CoNi_xO₁₉) using the co-precipitation method, based on the natural iron sand of the Loang Balok beach, Sekarbela District, Mataram, Indonesia. The synthesis was carried out with variations in the concentration of doping ions ($x = 0.0, 0.6, \text{ and } 1.0$). The characterization of the sample was completed using XRD, SEM-EDX, TEM. The XRD results showed that the sample had a hexagonal structure because it had a c / a value of 2.3 to 2.6. In contrast, SEM-EDX showed that the sample size of BaFe₁₂CoNiO₁₉ had reached the range of nanoparticles from 41 nm to 151 nm which was evenly distributed, with a composition of Ba = 12.22%; Fe = 49.1%; Co = 8.78%; Ni = 4.76%; and O = 21.37%, and slight impurities Cl = 3.77%.

INTRODUCTION

This research focuses on the synthesis of BaFe_{12-2x}CoNi_xO₁₉ based on natural iron sand to determine its structural properties. Furthermore, BaM (BaFe₁₂O₁₉) has been known to be a high-performance permanent magnetic material, theoretically possess a saturation magnetic of 72 em /g [1], the coercivity of 6700 Oe [2], Curie temperature of 502°C [3], good chemical stability, and corrosion resistance [4]. Besides, it has a hexagonal structure, with the same values for a and $b = 5.8920\text{\AA}$, while $c = 23.1830\text{\AA}$ was different [5].

Type-M hexaferrite MeFe₁₂O₁₉ (Me = Ba, Sr, Pb) is the earliest developed hexagonal ferrite class, which is also interesting to be studied because its magnetic properties are easily engineered according to the desired application [7]. However, this characteristic is modified by substituting Fe³⁺ ions with trivalent ions, including Cr, Al, Ga, In, Sc [8]. Besides, modifications are made by adding tetravalent ion combinations consisting of Ti⁴⁺, Ru⁴⁺, Zr⁴⁺, or Sn⁴⁺, with divalent varieties, such as varieties Ni²⁺, Co²⁺, Zn²⁺, Ti²⁺ or Sn²⁺ [9].

Barium M-hexaferrite in its application as a wave absorbent material must possess a low coercivity value, or be soft magnetic. Hence, substitution or drying is required. Moreover, there are two commonly used approaches for ionic exchanges. First, single-ion substitution approach, which has been conducted in previous studies, e.g., synthesized it by adding Ce doping [10], used La [11], adopted Eu [12], used Cu [13], Mn, and Ti, and utilized Sr and Mn [14]. The second, double ions method adopted in prior studies involving Co-Zn, Co-Mn, and Mn-Ni [15], Mn-Ti, Co-Ti, Ni-Ti, and Zn-Ti [16], and Co-Zn and Ni-Zn [17].

One possible technique used as co-precipitation contemporarily applied in the synthesis of inorganic compounds, based on the deposition of more than one substance together, after it passes the saturation point. This is widely employed by researchers, including the synthesis of BaM to determine its structural, electrical, and magnetic properties [18]; Determination of its magnetic properties [19]; Verifying the absorption properties of waves produced [20]; while ascertained the magnetic properties [21,22].

Many studies used the co-precipitation method due to its various advantages. Those advantages include comprising the requirement of low temperature, ease of particle size control; hence, the time needed is relatively shorter, and its ability to produce homogeneous particle size in the nano order. Doping applied as cobalt (Co) and nickel (Ni) metals,

included in period four transition elements, and precisely in group VIIIB elements. Furthermore, their horizontal similarity is greater than the vertical, the elements' nature picture was based on the horizontal group of each of the three, termed triads, according to the nomenclature of the best-known element. Therefore, there are iron, palladium, and platinum triads, respectively, known that Co and Ni tend to possess the same characteristics. Furthermore, some investigations employed the use of either metal as doping to reduce BaM properties, e.g., Ni [23,24]; Co-Ti alloys [25]; and Zr-Co [26].

METHODS

The synthesis of $\text{BaFe}_{12-x}\text{Co}_x\text{Ni}_x\text{O}_{19}$ was carried out with variations in the Co-Ni doping mole fraction, $x = (0.0; 0.6; \text{ and } 1.0)$. Meanwhile, Fe_3O_4 was dissolved in HCl, using a magnetic stirrer at $70\text{ }^\circ\text{C}$ for 30 minutes, and BaCO_3 was also diluted into HCl solution by using a magnetic hot plate stirrer at $70\text{ }^\circ\text{C}$ for 120 minutes. Furthermore, $\text{CoCl}_2 \cdot 6\text{H}_2\text{O}$ and $\text{NiCl}_2 \cdot 6\text{H}_2\text{O}$ were powdered for each mole fraction ($x = 0.0; 0.6; \text{ and } 1.0$) in H_2O , through the use of magnetic stirrers until they were completely dissolved or homogenized. Subsequently, all these solutions were mixed and stirred for 45 minutes until homogeneous. Therefore NH_4OH 6.5 M was dripped slowly until a precipitate was formed, and the sediments filtered with a filter paper and wash with distilled water until $\text{pH} = 7$ was achieved. Besides, the precipitates were dried at $80\text{ }^\circ\text{C}$ for 4 hours, and sequentially ground to the point where the smooth precursor is calcined at temperature variations ($T = 400, 600, 800 \text{ and } 1000\text{ }^\circ\text{C}$) and further characterized using XRD, SEM-EDX, TEM.

RESULTS AND DISCUSSION

Results from XRD Characterization

Characterization using XRD was performed on samples, BaM doping $x = 1.0$ ($\text{BaFe}_{10}\text{Co-NiO}_{19}$) mole fraction at $800\text{ }^\circ\text{C}$. The data obtained from XRD were X-ray diffraction intensity, and the two angles depicted in the graph showing the relationship and function, as shown in Fig. 1. The pattern also illustrated several parameters, e.g., scattering angle (2θ) and particle size (D) for variations in doping composition, including each -one as shown in Table 1.

TABLE 1. Lattice constants, c/a , unit cell volume and particle size of the $\text{BaFe}_{12-2x}\text{Co}_x\text{Ni}_x\text{O}_{19}$

Sample	Value $a = b$ (Å)	Value c (Å)	c/a	Cell volume (Å ³)	Particle Size (Å)
$x = 0.0$	5.0287	13.4346	2.671585	339.7317	296.48
$x = 0.6$	5.7591	13.7134	2.381171	454.8355	376.25
$x = 1.0$	5.8602	13.7453	2.345534	472.0403	401,85

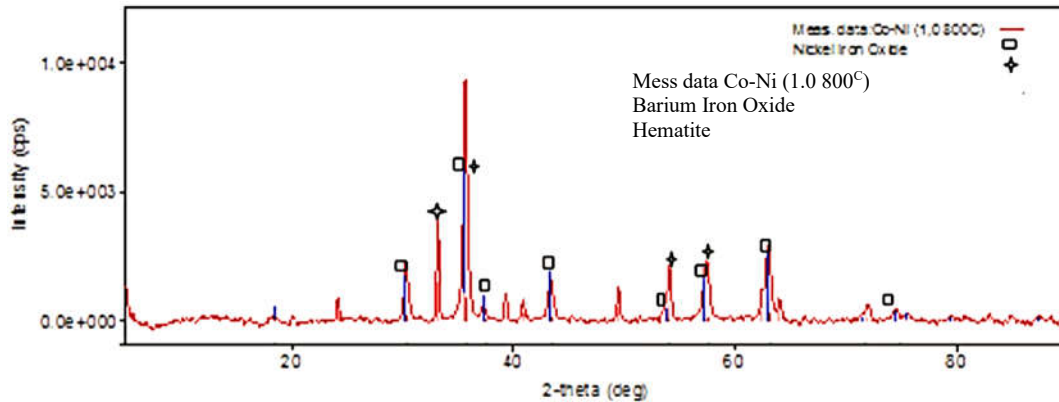


FIGURE 1. XRD pattern result of the $\text{BaFe}_{10}\text{Co-NiO}_{19}$.

The results are shown in Fig. 1, indicating that the dominant phase formed was Barium Iron Oxide ($\text{BaFe}_{12}\text{O}_{19}$) and Hematite (Fe_2O_3). Besides, the scattering angle data, interplanar distance, FWHM value, and particle size for each were listed in Table 1. Fig. 1 showed the formation of not only $\text{BaFe}_{12}\text{O}_{19}$ but also the Fe_2O_3 phase. According to [27], the presence of the latter is a natural phenomenon that occurs as a result of “in principle” iron oxide (Fe_3O_4) particles experiencing rapid oxidation. This is, however, unavoidable during synthesis, as other oxides or sub-oxides existed on the surface. This corresponds to a report of the Fe_2O_3 phase as stable for iron (III) oxide, derived from the heating process of the magnetite (Fe_3O_4) during synthesis [28]. Meanwhile, at temperatures of about 250 °C maghemite was formed, which dominated at 350 °C, while at 450 °C the composition of the phase began to decline, thus, at 550 °C, it changed into hematite, which prevailed at 700-800 °C [29]. Besides, to obtain a single-phase BaM, calcination must be carried out at temperatures above 800 °C, because previous research reported a single-phase being formed at 1100 °C and 1200 °C [30]. In Fig. 1 it is clear that the greater the amount of Co-Ni doping, the larger the particle size while the smaller c/a ratio [31].

Results of SEM-EDX Characterization

Characterization by SEM-EDX was carried out for $\text{BaFe}_{10}\text{Co-NiO}_{19}$ samples calcined at a temperature of 800 °C. The data of the distribution spectrum of the elements contained obtained in the form of graph and the number of sample elements in the percentage, as shown in Fig. 2. Fig. 2 and 3 show the results of SEM-EDX characterization for $\text{BaFe}_{10}\text{Co-NiO}_{19}$ samples that were calcined at 800 °C. Based on Fig. 2a and 2b, the particle size was in the nano order range, from 41 nm to 151 nm. Fig. 2. illustrates the morphology of the sample at a magnification of 20000 and 50000 times to look like evenly distributed grains or lumps, some of which overlap and form a pore.

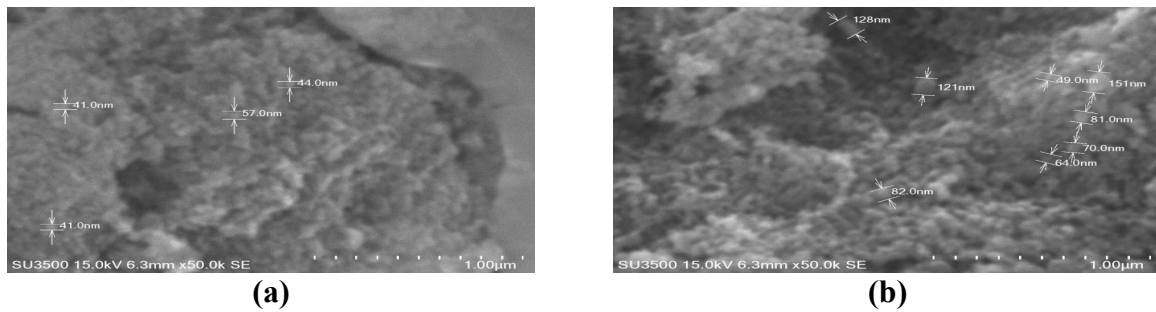


FIGURE 2. SEM results of $\text{BaFe}_{10}\text{Co-NiO}_{19}$ with a) 20000 and b) 50000 magnification

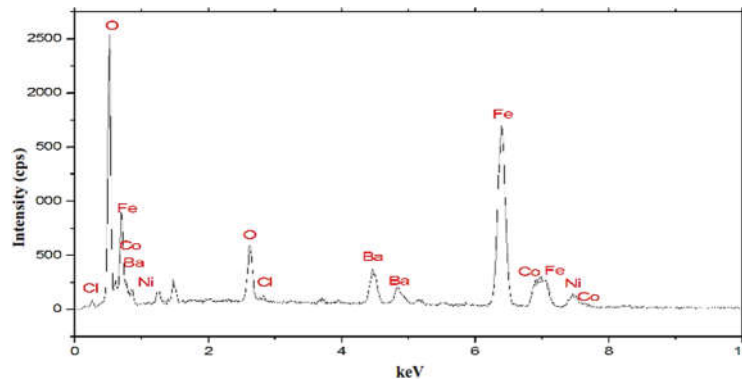


FIGURE 3. Composition diagram of $\text{BaFe}_{10}\text{Co-NiO}_{19}$

SEM image analysis has not been able to recognize each sample constituents directly, therefore, further characterization is required using EDX. The composition diagram of the $\text{BaFe}_{10}\text{Co-NiO}_{19}$ was shown, which indicated the elements in the composition of the sample to be Fe (49.1%), as shown, while O (21.37%), Ba (12.22%), Co (8.78%), Ni (4.76%), and little impurity of Cl (3.77%), followed respectively. Meanwhile, Co and Ni did not appear in the test using XRD because their percentage was relatively insignificant. However, the impurity (Cl) was derived during co-precipitation reactions, which did not evaporate entirely at 800 °C.

Results of TEM Characterization

Characterization with TEM was conducted as SEM-EDX on BaFe₁₀Co-NiO₁₉ calcined at 800 °C, and the data obtained are presented in Fig. 4.

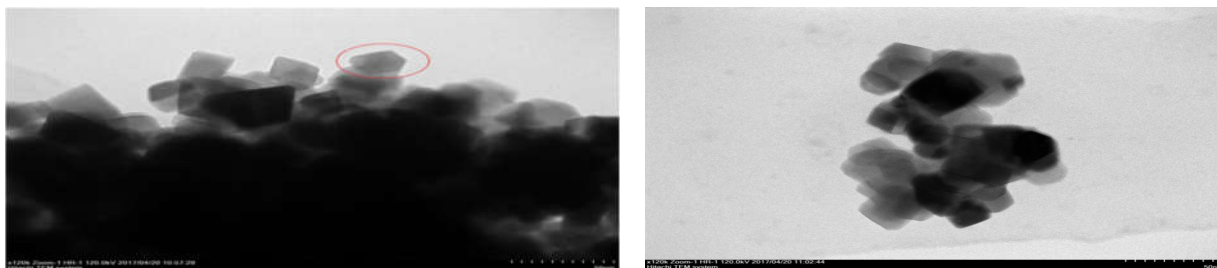


FIGURE 4. Results of TEM of the BaFe₁₀Co-NiO₁₉

Figure 4 shows the results of characterizing calcined samples at 800 °C, with the use of TEM, aimed at observing the barely visible crystal structure formed while using SEM-EDX, due to its higher resolution. Based on these images, hexagonal components were observed and circled in red lines. The structure formed in this sample was hexagonal because the less than 3.98 c/a ratio [32, 33]. This further strengthens the outcomes of XRD analysis, depicting hexagonal structures that were based on lattice constant ratio c/a , in the range of 2.3 to 2.6.

CONCLUSION

Based on the results of the research and discussion, the synthesis of natural iron sand based BaFe_{12-2x}Co_xNi_xO₁₉ samples resulted dominantly in barium iron oxide and hematite phases. Furthermore, it also possesses a hexagonal crystal structure, with $a = b = 5.8602$ Å, and $c = 13.7453$ Å, as well as particle size in the nano order range between 41 - 151 nm.

ACKNOWLEDGMENTS

Our sincere thanks are addressed to the RISTEKDIKTI team research for the financial support through contract number PTUPT: 1869/ UN18. L / PP/ 2019 and all of the people who have helped this research.

REFERENCES

1. Radwan, M., Rashad, M.M., and Hessien, M.M. *J. Mater. Process. Technol.* 181, 106 (2007).
2. G. Carreno, T., Morales, M.P., and Serna, C.J. *Mater. Lett.* 43, 97 (2000).
3. Cernea, M., Sandu, S.G., Galassi, C., Radu, R., and Kuncser, V. *J. Alloys Compd.* 561, 121 (2013).
4. Tang, X. *Journal of Material Science. ISSN*, 0022-2461 (2005).
5. Mallick, K. K., Shepherd, P. dan Green, R. J. *Journal of the European Ceramic Society, Vol. 27, page. 2045–2052* (2007)
6. Syamsir, A. *Journal of Physics Unand*, 1(1) (2012).
7. Awawdeh, M., I. Bsoul, and S. H. Mahmood. *Journal of Alloys and Compounds* 585: 465-473 (2014).
8. Dhage, V. N., Mane, M. L., Babrekar, M. K., Kale, C. M., & Jadhav, K. M. *Journal of Alloys and Compounds*, 509(12), 4394-4398 (2011).
9. Zhang, W., Bai, Y., Han, X., Wang, L., Lu, X., Qiao, L. *Journal of Alloys and Compounds*, 546, 234-238 (2013).
10. Chang, S., Kangning, S., & Pengfei, C. *Journal of Magnetism and Magnetic Materials*, 324(5), 802-805 (2012).
11. Li, C. J., Wang, B., & Wang, J. N. *Journal of Magnetism and Magnetic Materials*, 324(7), 1305-1311 (2012).
12. Khademi, F., Poorbafrani, A., Kameli, P., & Salamati, H. *Journal of superconductivity and novel magnetism*, 25(2), 525-531 (2012).
13. Baykal, A., Güngüneş, H., Sözeri, H., Amir, M., Auwal, I., Asiri, S., Demir Korkmaz, A. *Ceramics International*, 43(17), 15486–15492 (2017).
14. Soehada. *Jurnal Sains Material Indonesia* 15(4); 192-195 (2014).

15. Susilawati, A. Doyan, Khalilurrahman. *AIP Conference Proceedings* 1801, 040007 (2017).
16. Sözeri, H., Deligöz, H., Kavas, H., & Baykal, A. *Ceramics International*, 40(6), 8645-8657 (2015).
17. Agustianto, R., & Widyastuti, W. *Jurnal Teknik ITS*, 3(1), F108-F112 (2014).
18. M. N. Akhtar, M. A. Khan. *Article in Ceramics International* (2018).
19. Arief Setiadi, E., Shabrina, N., Retno Budi Utami, H., Fadhilah Fahmi, N., Kato, T., Iwata, S., & Suharyadi, E. *Indonesian Journal of Applied Physics*, 3(1), 1-8 (2013).
20. Khan, K., & Rehman, S. *Materials Research Bulletin*, 50, 454-461 (2014).
21. Tawainella, R. D., Riana, Y., Fatayati, R., Kato, T., Iwata, S., & Suharyadi, E. *Jurnal Fisika Indonesia*, 18(52) (2015).
22. Hedayati, K., Azarakhsh, S., & Ghanbari, D. *Journal of Nanostructures*, 6(2), 127-131 (2016).
23. R. Sharma, P. Thakur. V. Sharma. *Journal of Alloys and Compounds* 684 (2016).
24. Dawar, N., Chitkara, M., Sandhu, I. S., Jolly, J. S., & Malhotra, S. *Cogent Physics*, 3(1), 1208450 (2016).
25. Wei, L., Che, R., Jiang, Y., Yu, B. *Journal Environ Sci (China) Suppl 1: S27-31* (2013).
26. Susilawati, Doyan, A., and Munib M. 2015. Synthesis by co-precipitation method and characterization of Nickel-doped Barium M-Hexaferrite (BaFe₁₂O₁₉). Proceeding ICMSE ISBN 9786021570425.
27. Puzan, M., Kato, T., Iwata, S., & Suharyadi, E. 2013. Effect of Grain Size and Crystal Structure on Magnetic Properties of Magnetic Nano particles (Fe₃O₄). *Prosiding gPertemuan ilmiah XXVII HFI Jateng dan DIY*.
28. G. Mu, N. Chen, X. Pan, *Materials Letters* (2008).
29. S. Simms, V. Fusco. *The Institution of Engineering and Technology* (2006).
30. P.A. Mariño-Castellanos, J.C. Somarriba-Jarque. J. Anglada-Rivera. *Physica B: Condensed Matter Volume 362, Issues 1-4*.
31. Susilawati, Doyan, A., Taufik, M., Wahyudi, Ryantin G., E., Fitriani, A., Nazarudin. *Journal Materials Science Forum*, 966: 282-289 (2019).
32. T.R. Wagner, Preparation and crystal structure analysis of magnetoplumbite type BaGa₁, *J. Solid State Chem.* 136 (1998) 120-124 (2019).
33. Susilawati, Doyan, A., Khair, H., Taufik, M., Wahyudi, *Journal of Physics: Conf. Series* 1011 012009 (2018).